Mandible shape modeling using the second eigenfunction of the Laplace-Beltrami operator

Seongho Seo[a], Moo K. Chung[abc], and Houri K. Vorperian[d]

[a]Department of Brain and Cognitive Sciences, Seoul National University, Korea
[b]Department of Biostatistics and Medical Informatics,
[c]Waisman Laboratory for Brain Imaging and Behavior,
[d]Vocal Tract Development Laboratory, Waisman Center,
University of Wisconsin, Madison, WI, USA.

ABSTRACT

The second Laplace-Beltrami eigenfunction provides an intrinsic geometric way of establishing natural coordinates for elongated 3D anatomical structures obtained from imaging images. This approach is used to establish the *centerline* of the segmented human mandible and provides automated anatomical landmarks across subjects. These landmarks are then used to quantify the growth pattern of the mandible between ages 0 and 20.

1. INTRODUCTION

The skull consists of the craniofacial complex and the mandible. The craniofacial complex includes the cranium and the face. Although the cranium and the face are closely located anatomically, they have different growth patterns.[1] The cranium follows a neural growth pattern where it is considered to be very close to its mature size by about the age of six years. The face, on the other hand, specifically the middle and lower anterior regions of the face (eyes to chin), follows the general somatic or skeletal growth curve and continues to grow till about age 18 years. The growth of the mandible, a U-shaped bone (superior view) that forms the lower jaw, contributes to the maturation of the face. It consists of a body and a pair of rami that articulate with the cranium at the temporomandibular joints. So, while its vertical growth appears to follow a somatic or skeletal growth pattern, its lateral growth is expected to follow more of a neural growth pattern particularly at the condylar level (level of temporomandibular joint) but not necessarily at the lingual (tongue) level. The growth of the human mandible has been characterized to consist of a general increase in size as well as remodeling where there is simultaneous growth forward and downward,[2–4] and also bilateral growth.[5] The mandible is a moving bone, and its growth and remodeling is dependent on the growth and biomechanical forces of all other component structures (bony and soft tissue structures) in the craniofacial complex. Thus the purpose of this paper is to quantitatively characterize the 3D growth of the mandible while accounting for the gender difference using an intrinsic geometric approach.

For a 3D growth pattern analysis of the mandible, it is desirable to represent mandibular shape in a concise form while preserving essential shape properties. As 3D models become common in many disciplines, curve skeleton or *centerline* has been developed for a wide range of applications, since it captures the essential topology as a 1D representation of 3D object.[6] Recently, several methods based on the Reeb graph has been developed to extract the centerline.[7,8] The Reeb graph captures the topology of an arbitrary manifold by describing the connectivity of the level sets of the function defined on the manifold. Since Reeb graph of the second eigenfunction of Laplace-Beltrami operator captures the global geometry and is pose-invariant, Shi et al.[8] proposed to use it in computing skeleton of a simply connected 2D surface patch.

In this paper, we propose to extract the centerline of mandible using the level sets of second eigenfunction of the Laplace-Beltrami operator. We then apply the extracted centerline shape to characterize the growth pattern of the mandible.

Send correspondence to Moo K. Chung. 1500 Highland Ave. Madison, WI. 53705. USA. Moo K. Chung: E-mail: mkchung@wisc.edu

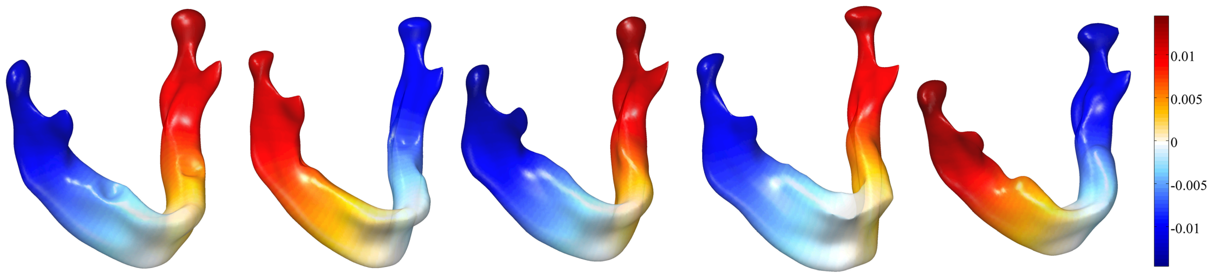

Figure 1. The second eigenfunction ψ_1 for different mandibles. ψ_1 for a elongated object is a smooth monotonic function increasing from one part of the symmetry to the other part.

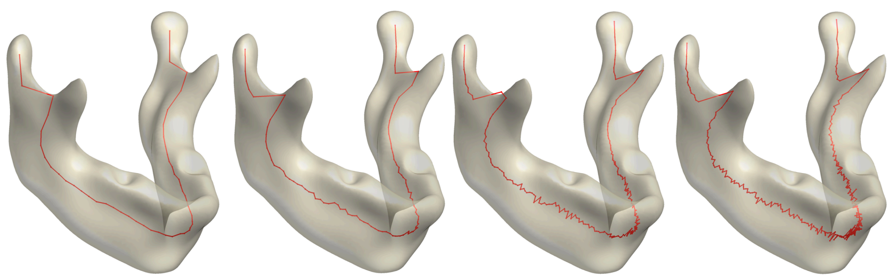

Figure 2. The centerline of a mandible surface with different number of level bands k: 50, 100, 200 and 300. As k increases, the centerline introduces more noise.

2. IMAGE ACQUISITION AND PREPROCESSING

Our imaging data set was composed of 71 subjects (41 males and 38 females). The age distribution was 11.42 ± 5.54 years for the female group, and 9.69 ± 5.71 years for the male group. The CT images were obtained using GE multi-slice helical CT scanners. The CT scans were acquired directly in the axial plane with a 1.25 mm slice thickness, matrix size of 512×512 and 15–30 cm field of view (FOV), and image resolution in the range of 0.29 to 0.59 mm.

CT scans were converted to DICOM format and Analyze 8.1 software package (AnalyzeDirect, Inc., Overland Park, KS) was used in segmenting binary mandibular structure by thresholding image intensity. The binary segmentations were converted to surface meshes via the marching cubes algorithm. To reduce mesh noise, we applied heat kernel smoothing[9] with $\sigma = 0.5$ to all 79 mandibular surfaces. The heat kernel was explicitly constructed as a series expansion of the eigenfunctions of the Laplace-Beltraimi operator. The Fourier coefficients for the finite expansion of heat kernel smoothing were estimated using the least-squares method. The degree of expansion was fixed at 230.

3. CENTERLINE OF MANDIBLE

We solved $\Delta f = \lambda f$ to get the second eigenfunction ψ_1 on the smoothed mandible surface $\mathcal{M}$, where Δ is the Laplace-Beltrami operator on the smoothed surface. Since the closed form expression for the eigenfunctions of the Laplace-Beltrami operator on an arbitrary surface is unknown, the eigenfunctions were numerically computed using the Cotan formulation.[8,10,11] The `MATLAB` code is given at http://brainimaging.waisman.wisc.edu/~chung/lb. As shown in Fig. 1, the second eigenfunction ψ_1 is a smooth monotonic function increasing from one part of the symmetry to the other part.

The mandible centerline was obtained by connecting the centroids of the successive level contours of ψ_1.[7,8] The centroids were computed as the average of all points p in the same level contour $\psi(p) = c$ for some fixed c. Due to discrete nature of data, stable results were difficult to obtain. We therefore opted to average all points p in the same level band $c - \epsilon \leq \psi(p) \leq c + \epsilon$ for small ϵ. Fig. 2 shows the resulting centerline of a

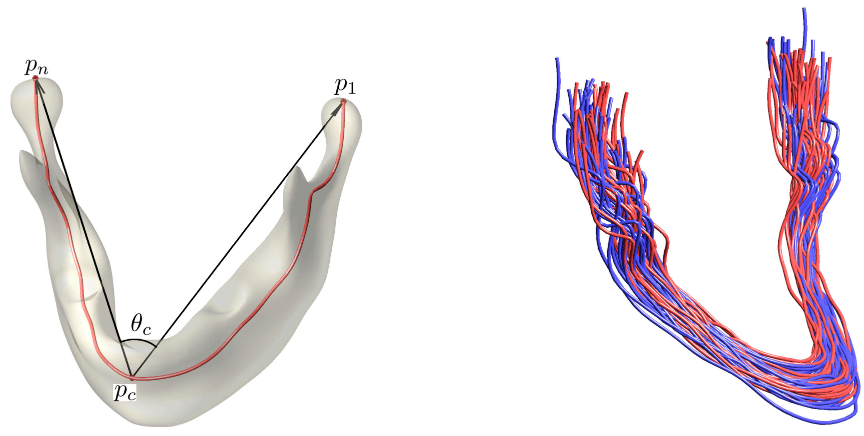

(a) (b)

Figure 3. (a) From the centerline model, we obtain the angle θ_c between the tips p_1 and p_n of Condylar process, which are the end points of the centerline, and the the center of the symmetry p_c, which is obtained as the point with the smallest z coordinate value. (b) Centerlines of all subjects (female =red, male = blue). Each centerline was extracted from 100 level bands and further smoothed using the 29-th degree cosine series representation.

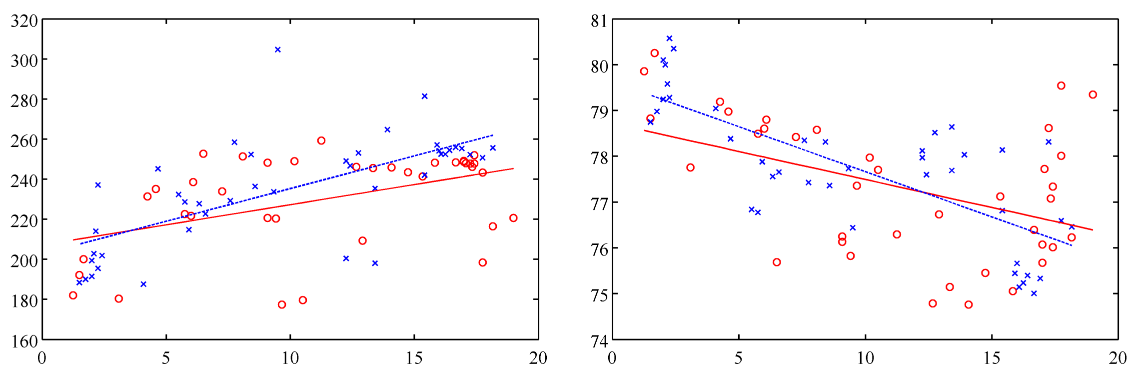

(a) length (mm) (b) angle (°)

Figure 4. Linear regression of length l_c and angle θ_c of centerline on age (years). Red 'o' marks and solid line are the female group, and blue 'x' marks and dashed line are the male group.

mandible surface for various number of bands k. We have fixed k to be 100 for all mandibles. A k increases, the centerline fluctuates more rapidly and introduces noise. To overcome this problem, we used the *cosine series representation*.[12] By representing the coordinates as linear combinations of smooth basis functions, the cosine representation enables us to get more smooth centerline reducing the fluctuation noise. The cosine series representation of all subjects are shown in Fig. 3b. The `MATLAB` implementation of the cosine series representation is given at http://brainimaging.waisman.wisc.edu/~chung/tracts.

To quantify mandibular growth, we used two morphometric measures: length l_c of the mandible and the angle θ_c between the two Condylar processes p_1 and p_n, and the center of symmetry p_c (Fig. 3a). The length l_c is the total length of the centerline between the tips of Condylar processes p_1 and p_n and it is approximated as $l_c = \sum_{i=2}^{n} \|p_i - p_{i-1}\|$. The angle θ_c was computed using $\theta_c = \cos^{-1} \frac{\langle p_1 - p_c, p_n - p_c \rangle}{\|p_1 - p_c\| \|p_n - p_c\|}$ and measured in degrees.

4. MANDIBLE GROWTH MODEL

We measured the length and angle from the centerline model. The length distribution was 230.05 ± 24.03 mm for females and 234.23 ± 27.48 mm for males (Fig. 4a). The angle was $77.32 \pm 1.53°$ for females, and $77.72 \pm 1.50°$ (Fig. 4b) for males. We fitted a linear growth model of the form

$$\texttt{length, angle} = \beta_0 + \beta_1\,\texttt{gender} + \beta_2\,\texttt{age} + \beta_3\,\texttt{gender} \cdot \texttt{age}$$

and tested for the significance of the gender or age terms without the higher order interaction term. Fig. 4a and 4b show significant length increase and angle decrease in males relative to females at later age range. We tested the effect of age term β_2 while accounting for gender difference and found highly significant results for mandibular length and angle (length: p-value $= 2.63 \times 10^{-6}$, $F_{1,76} = 25.80$; angle: p-value$= 1.34 \times 10^{-6}$, $F_{1,76} = 27.56$). As noted in Fig. 4a and 4b, the rate of length increase and angle decrease appeared to be different for males and females. We therefore tested the significance of the interaction term β_3 to determine the significance of the rate difference. Possibly due to smaller sample size relative to intersubject variability, significance is weak (length: p-value$= 0.15$; $F_{1,75} = 2.10$, angle: p-value$= 0.14$, $F_{1,75} = 2.25$). We also tested the gender effect β_1 while accounting for age differences. The length shows weakly significant gender difference while the angle does not (length: p-value$= 0.08$, $F_{1,76} = 3.21$; angle: p-value$= 0.66$,$F_{1,76} = 0.20$).

ACKNOWLEDGMENTS

This work was supported by NIH-grant R01 DC6282 from the National Institute of Deafness and other Communicative Disorders, a core grant P-30 HD03352 to the Waisman Center from the National Institute of Child Health and Human Development, and WCU-grant from the government of Korea to the Department of Brain and Cognitive Sciences, Seoul National University. We thank Dongjun Chung, Lindell R. Gentry, Mike S. Schimek, Katelyn J. Kassulke and Reid B. Durtschi for assistance with image acquisition and segmentation.

REFERENCES

[1] Scammon, R. E., "The measurement of the body in childhood," in [*The measurement of man*], Harris, J. A., Jackson, C. M., Patterson, D. G., and Scammon, R. E., eds., 173–214, University of Minnesota Press, Minneapolis (1930).

[2] Scott, J. H., [*Dento-facial Development and Growth*], Pergamon Press, Oxford (1976).

[3] Smartt Jr., J. M., Low, D. W., and Bartlett, S. P., "The pediatric mandible: I. A primer on growth and development," *Plast. Reconstr. Surg.* **116**, 14e–23e (July 2005).

[4] Walker, G. F. and Kowalski, C. J., "On the growth of the mandible," *American Journal of Physical Anthropology* **36**, 111–118 (January 1972).

[5] Enlow, D. H. and Hans, M. G., [*Essentials of Facial Growth*], W.B. Saunders Company, Philadelphia (1996).

[6] Cornea, N. D., Silver, D., and Min, P., "Curve-skeleton properties, applications, and algorithms," *IEEE Transactions on Visualization and Computer Graphics* **13**(3), 530–548 (2007).

[7] Lazarus, F. and Verroust, A., "Level set diagrams of polyhedral objects," in [*Proceedings of the fifth ACM symposium on Solid modeling and applications*], 130–140 (1999).

[8] Shi, Y., Lai, R., Krishna, S., Sicotte, N., Dinov, I., and Toga, A. W., "Anisotropic Laplace-Beltrami eigenmaps: Bridging Reeb graphs and skeletons," in [*Proceedings of Mathematical Methods in Biomedical Image Analysis (MMBIA)*], 1–7 (2008).

[9] Seo, S., Chung, M. K., and Voperian, H. K., "Heat kernel smoothing using Laplace-Beltrami eigenfunctions," in [*13th International Conference on Medical Image Computing and Computer Assisted Intervention (MICCAI 2010)*], *Lecture Notes in Computer Science (LNCS)* (2010, in press).

[10] Chung, M. K., *Statistical Morphometry in Neuroanatomy*, PhD thesis, McGill University (2001).

[11] Qiu, A., Bitouk, D., and Miller, M. I., "Smooth functional and structural maps on the neocortex via orthonormal bases of the Laplace-Beltrami operator," *IEEE Transactions on Medical Imaging* **25**, 1296–1396 (2006).

[12] Chung, M. K., Adluru, N., Lee, J. E., Lazar, M., Lainhart, J. E., and Alexander, A. L., "Cosine series representation of 3D curves and its application to white matter fiber bundles in diffusion tensor imaging," *Statistics and Its Interface* **3**, 69–80 (2010).